Electron spin polarization and detection in InAs quantum dots through *p*-shell trions

S. G. Carter, Ş. C. Bădescu, and A. S. Bracker
Naval Research Laboratory, Washington, DC 20375-5322, USA

(Received 16 September 2009; revised manuscript received 10 November 2009; published 8 January 2010)

We perform two-color time-resolved spectroscopy of spin dynamics in an ensemble of InAs quantum dots, demonstrating that an electron spin polarization in negatively charged quantum dots can be efficiently generated or detected with pulses tuned to *p*-shell trions. Due to the polarization selection rules and exchange splitting of the electron spin triplet and singlet trion states, the absorption probability of circularly polarized light depends strongly on the spin state of the resident electron in the quantum dot. This leads to spin selective excitation of electrons to the *p*-shell trion states, generating a spin polarization in the ensemble of unexcited resident electrons. Manipulating spin states through the excited trion states allows for separation of the excitation wavelength from the emission wavelength for control of the spatial extent of the excited-state wave function.

DOI: 10.1103/PhysRevB.81.045305 PACS number(s): 78.67.Hc, 78.47.D−, 72.25.Fe

I. INTRODUCTION

An electron or hole spin in a semiconductor quantum dot (QD) is a strong candidate as a quantum bit for quantum information applications. Optical manipulation of spin states has been of particular interest since it can be performed on ultrafast time scales, it couples the spin qubit to photon qubits, and it can spectrally or spatially select different QDs. Much of the previous work in this area has relied on the lowest charged exciton (trion) state, in which an electron-hole pair is generated in the conduction and valence *s* shells of the QD. Resonant or near-resonant excitation of this lowest-energy trion state has been quite productive, with several recent demonstrations of spin-state initialization,[1,2] time-resolved single-spin detection,[3] and fast spin rotation.[4–6]

Using excited trion states can provide additional flexibility and functionality. One advantage of optical manipulation with excited states is that the wavelength of the excitation laser is well separated from the QD emission wavelength, preventing scattered laser light from overwhelming emission.[7] Another benefit of using excited states is having multiple transitions with different functions. In the coupled QD system of Ref. 8, use of the triplet trion states (excited spin states) was essential to produce a lambda system for spin manipulation as well as cycling transitions for readout. Also, control of the orbital wave function through excited states can be used to control coupling to nearby QDs. A recent theoretical study showed that the extended orbital wave functions of excited-state trions can be used to entangle two electron spins in two nearby QDs that are uncoupled in the ground states.[9] In this work, we show that particular excited trion states in single QDs, *p*-shell trions (with an *s*-shell electron, a *p*-shell electron, and a *p*-shell hole), can be used to manipulate and detect electron spin states.

There have been a number of previous studies of the excited trion states in QDs using photoluminescence (PL).[7,10–19] These studies give information on the energies and polarizations of the different transitions, and many have been able to infer a resident electron spin polarization based on luminescence polarization. A few studies have also measured the time-resolved carrier dynamics[11,12,17,19] and temporal correlation of emitted photons.[7,14] These time-resolved luminescence studies provide information on trion dynamics and relaxation but do not directly measure the resident electron spin state.

Using two-color time-resolved Faraday rotation and ellipticity (TRFR and TRFE), we directly polarize and probe the resident electron spins in an ensemble of InAs QDs using the *p*-shell trion states. A circularly polarized pump pulse preferentially excites QDs with a particular resident electron spin polarization [see Figs. 1(a) and 1(b)]. After excitation the resident electrons in unexcited QDs are then primarily of the opposite spin orientation. A linearly polarized probe pulse measures this resident spin polarization, which precesses in the applied magnetic field as a function of probe delay. Spin selectivity comes from the polarization selection rules of the *p*-shell trion states and the significant electron-electron exchange splitting between the triplet and singlet states. We observe this selectivity by examining TRFR and TRFE as a function of pump and probe photon energy. When the probe

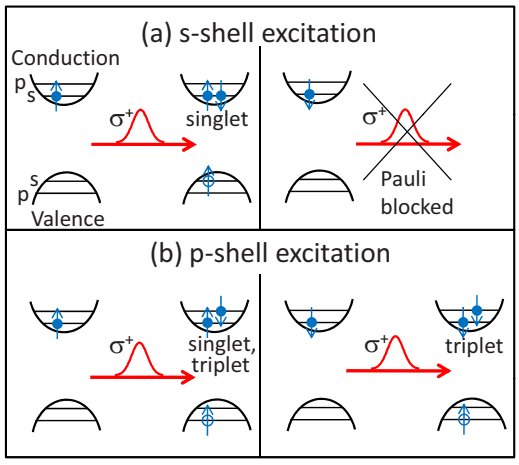

FIG. 1. (Color online) Electron- and hole-energy levels in a quantum dot, showing spin selectivity in the excitation of (a) *s*-shell trions and (b) *p*-shell trions for different initial spin states. Spin selectivity is provided by Pauli blocking in the *s* shell and by different energies and dipole moments of singlet and triplet states in the *p* shell.

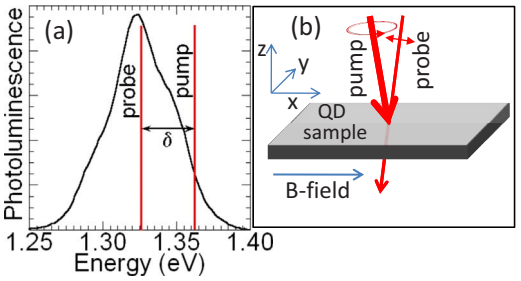

FIG. 2. (Color online) (a) Photoluminescence of the quantum dots. The vertical lines represent the pump and probe. (b) Experimental geometry for pump-probe experiments.

photon energy is fixed at the *s*-shell trion and the pump is scanned to higher photon energies, a clear peak in the spin polarization is observed at the expected *p*-shell trion energy. We also fix the pump at the *s*-shell trion and scan the probe to observe a peak in the detection of the spin polarization at the *p*-shell trion. These results are a step toward greater functionality in optical control of spin states in quantum dots.

II. EXPERIMENT

The QD sample consists of 20 layers of InAs QDs, grown by molecular-beam epitaxy through Stransky-Krastanov self-assembly. The QDs are partially capped with GaAs and the remaining InAs is flushed away to produce a truncated disk structure of height 2.5 nm and lateral dimension of 10–20 nm.[20] The QD layers are separated by 30 nm GaAs barriers, and the QD areal density per layer is estimated at $\sim 1 \times 10^{10}$ cm^{-2}. The sample is *n* doped with tellurium, making a significant fraction of the QDs charged with a single electron. Figure 2(a) displays the PL of the QDs at ~5 K, with a full width at half maximum of ~50 meV due to varying QD sizes. Emission from the *p*-shell states cannot be resolved due the large energy variation in the *s*-shell states.

Using pump-probe TRFR and TRFE [Fig. 2(b)], these *p*-shell states can be resolved. The pump-induced rotation or ellipticity of a linearly polarized probe pulse measures only those QDs with energy levels near the probe photon energy, which has a bandwidth of ~1 meV (1.8 ps pulse length). Ellipticity (rotation) corresponds to a difference in the amplitude (phase) of the σ^+ and σ^- components of the transmitted probe, giving sensitivity to spin. A circularly polarized pump pulse (also with a bandwidth of ~1 meV) can only affect the probe polarization when the pump is resonant with energy levels of the subset of QDs measured by the probe. The delay of the probe relative to the pump gives picosecond time resolution, and the pulses are repeated at a rate of 81 MHz. The pump (probe) pulse is focused down to a diameter of ~80 μm (~50 μm) with an average intensity of ~60 W/cm^2 (~10–20 W/cm^2). These intensities are kept well below saturation in order to avoid complicating effects such as "mode locking"[21] and the accompanying nuclear-spin polarization effects that have previously been observed in this QD sample.[22]

Figure 3(a) displays the TRFE with the probe at a photon energy of 1.326 eV for two different pump detunings δ_{pump}

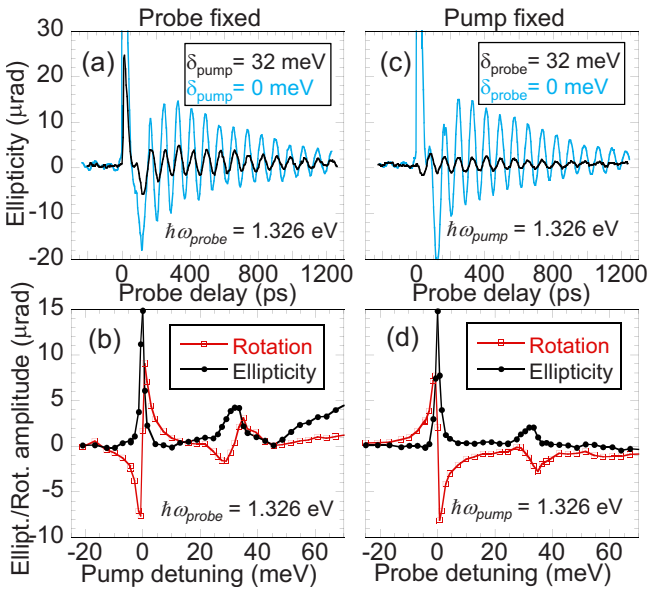

FIG. 3. (Color online) [(a) and (c)] TRFE signal vs probe delay for degenerate pump probe and for a detuning of 32 meV. [(b) and (d)] TRFR and TRFE amplitudes vs pump/probe detuning. The probe is fixed at $\hbar\omega_{probe}$=1.326 eV for (a) and (b), and the pump is fixed at $\hbar\omega_{pump}$=1.326 eV for (c) and (d).

$=\hbar\omega_{pump}-\hbar\omega_{probe}$. At the center of the PL, the probe primarily should be tuned to *s*-shell trions. An external magnetic field of 2 T is applied perpendicular to the optical axis (Voigt geometry) in order to observe precession of the electron spins. For degenerate pump probe (δ=0), where both are primarily tuned to *s*-shell trions, there are three different components due to neutral excitons, trions, and electrons. The neutral exciton (from uncharged QDs) gives the sharp signal near zero delay followed by a heavily damped oscillation due to the asymmetric exchange splitting. Trions give a simple exponential decay due to the lifetime of ~500 ps, and electron spins give the clear oscillating signal at 12 GHz due to precession in the magnetic field. Pumping at higher energies near the *p*-shell (δ_{pump}=32 meV) gives similar behavior with a smaller amplitude. One might also expect to observe dynamics of the excited trion states when pumping at high photon energies. Signals from the excited states may appear very similar to the neutral exciton and trion components, and many of the excited states relax quickly to the *s* shell, making it difficult to distinguish between them.

Here, we focus exclusively on the signal due to precessing electron spins. Interestingly, this signal is due to electrons that are *not* excited by the pump pulse. The pump pulse preferentially excites trions in quantum dots when the resident spin is of a particular orientation. Electron spins in the unexcited QDs are left with the opposite orientation. One might expect that trion recombination will strongly affect this electron spin polarization. However, in a significant Voigt magnetic field, precession of the electron spin during the trion lifetime means that recombination returns the electron spins with a random phase compared to unexcited precessing electron spins. The effect of recombination on the electron spin polarization thus averages out to zero, leading to a long-lived electron spin polarization.[23–25] The single-

spin coherence time in this sample has previously been measured to be 100–200 ns at 3 T.[22] The observed decay time of ~600 ps in Fig. 3(a) is due to inhomogeneity of the g factors in the QD ensemble. Signals at negative delays due to mode locking are weak at the low powers used in these experiments and have only been observed when pumping in the s shell. Additionally, no obvious signatures of nuclear-spin effects have been observed under these conditions.

Both the TRFE and TRFR are measured for a series of pump detunings from the fixed probe, and the electron spin component is fitted to an exponentially decaying cosine. The amplitudes are plotted in Fig. 3(b), displaying a strong resonance near zero detuning, a weaker resonance at ~30 meV, and features at higher energies starting at ~50 meV. The TRFR shows essentially the same features as TRFE but with dispersive features instead of absorptive. The focus of the discussion is on the TRFE as it gives a simpler spectrum while the TRFR amplitude provides a complementary spectrum that is antisymmetric about each resonance.[22] The zero detuning resonance is due to excitation of the s-shell singlet trion and its width (1.7 meV) corresponds to the spectral overlap of the pump and probe. We attribute the resonance at ~30 meV to the p-shell singlet and triplet trion states. The resonance is quite broad (8 meV) due to variation in the s-p splitting but the integrated signal is roughly the same as for the s-shell resonance. The decay time and phase of the electron spin signal are about the same when pumping in the s shell or p shell, as seen in Fig. 3(a). The higher energy features, which tend to blur together to form a continuum, will not be discussed here.

We also show that the electron spin state can be probed through the p-shell trions in Figs. 3(c) and 3(d), for which the pump is now fixed in the s shell at 1.326 eV. The TRFE signal vs probe delay is plotted in Fig. 3(c) with the probe in the s shell ($\delta_{probe}=\hbar\omega_{probe}-\hbar\omega_{pump}=0$) and in the p shell ($\delta_{probe}=32$ meV). The electron spin signal is smaller when probing in the p shell but has a similar phase and decay time. Figure 3(d) displays the spectral dependence of the probe. There is a strong s-shell resonance near the pump and a weaker p-shell resonance 32 meV higher, with much less signal at higher energies. The ability to probe the electron spin state through the p shell is possible for the same reason spin polarization is possible: electron spin selective trion transitions with circularly polarized light. An electron spin polarization results in more absorption (refraction) for one-photon helicity than the other, resulting in ellipticity (rotation) of the linearly polarized probe.

By varying both the pump and probe photon energies (taking time-resolved scans at each pump/probe combination), we produce a two-dimensional (2D) map of the excitation and detection of the resident spin polarization. This map, displayed in Fig. 4, is lower resolution than the scans in Figs. 3(b) and 3(d), but the main features are clear. The signal is strongest along the diagonal, for which the pump and probe are degenerate. Parallel to the diagonal but at a probe energy ~30 meV higher is a weaker signal, which corresponds to pumping the electron spin through the s-shell trion and probing through the p-shell trion. There is also a parallel feature about 30 meV below the diagonal, which corresponds to pumping electron spins through the p-shell trion and probing through the s-shell trion. This feature is surrounded by a near continuum, particularly for the highest pump photon energies. At these energies, the pump can excite into multiple excited trion states, so the probe can detect electron spins over a wide range of energies, including both the s-shell and p-shell trions.

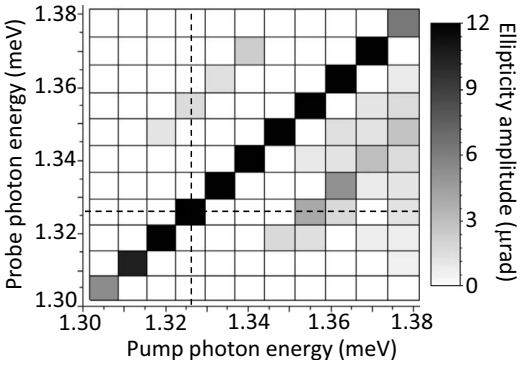

FIG. 4. Grayscale intensity map of the TRFE amplitude vs pump and probe photon energies. The horizontal and vertical dashed lines represent the scans taken in Figs. 3(b) and 3(d). The intensity scale is saturated for many points along the diagonal so that low intensity points can be seen.

III. ANALYSIS

To understand the origin of the electron spin polarization and detection, consider the energy levels of a negatively charged QD. Figure 5 shows the electron spin states (e_s), the trion states, and the allowed transitions between them for σ^+ excitation. The lowest trion state is an electron singlet with both electrons in the s-orbital state (S_s). The next trion state, labeled $p \leftrightarrow s$ is optically forbidden for QDs with inversion symmetry as it excites one carrier (either electron or hole) to

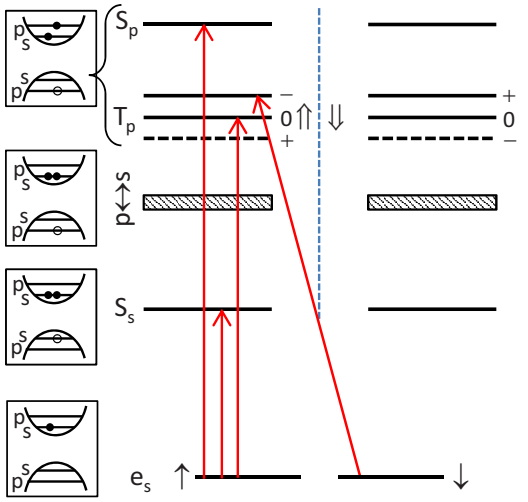

FIG. 5. (Color online) Energy levels of a negatively charged QD with the electron and hole energies shown separately to the left. The trions levels are divided left and right by the hole orientation, ⇑ and ⇓. Arrows show allowed transitions for σ^+ excitation with the spin states oriented along the optical axis.

the s shell and one to the p shell. The next excited states (T_p, S_p) contain one electron in the p shell, one electron in the s shell, and a hole in the p shell. The separation energy from the S_s is dominated the single-particle quantization energies of an electron and a hole. These excited states can have an electron-electron triplet (T_p) or singlet (S_p) spin structure, with a separation between them given by the electron-electron exchange energy Δ_{ee}. The triplet states have a fine structure due to the presence of electron-hole exchange. This diagram displays the electron spin states oriented along the optical axis (z) to simplify the selection rules. This picture works well during the excitation process since the pulse length (~2 ps) is much shorter than the electron precession period (83 ps).

We make the assumption for all of the trion states that only the spin-selective excitation generates the electron spin polarization. Excitation of a trion in a QD depolarizes the resident electron spin after recombination. The electron spin polarization comes from QDs that are *not* excited by the pulse. This is in contrast to several studies in which circularly polarized excitation in the wetting layer or barrier layers resulted in spin polarization.[12,17–19,26,27] In these previous experiments, excitation did not depend on the spin orientation of the resident QD electrons. Rather, relaxation and recombination of the spin-polarized, optically excited carriers resulted in a resident spin polarization. These experiments were performed either without a magnetic field, with a Faraday magnetic field, or with a very small Voigt magnetic field, none of which leads to significant spin precession during recombination. For a strong Voigt magnetic field, recombination should leave electron spins unpolarized.[23–25]

We also assume the electron spins are unpolarized before each pump pulse. For individual spins this assumption may be invalid since the individual spin coherence time is longer than the pulse repetition period. However, the ensemble spin polarization is nearly zero before each pulse due to inhomogeneity in the spin precession frequency, giving no significant negative delay signal in Fig. 3(a). These assumptions greatly simplify calculation of the electron spin polarization. The degree of spin polarization for a QD is only determined by the probability of the laser pulse to excite a spin-up electron vs a spin-down electron, $w_{\uparrow,n} - w_{\downarrow,n}$, where n is a particular trion state. These excitation rates are determined by the trion linewidths γ_n, by the spectral distribution of the laser (taken below as Gaussian), and by the dipole matrix elements μ_n of the transitions[28]

$$w_{\uparrow,n} - w_{\downarrow,n} \propto \int d\omega e^{-(\omega-\omega_0)^2/2\sigma^2} \frac{\gamma_n(|\mu_{\uparrow,n}|^2 - |\mu_{\downarrow,n}|^2)}{(\omega-\omega_n)^2 + \gamma_n^2}. \quad (1)$$

The spectral width and center of the laser pulse are σ and ω_0, respectively. If the processes that eliminate $|\uparrow\rangle$ from the ensemble dominate $(\Sigma_n w_{\uparrow,n} > \Sigma_n w_{\downarrow,n})$ then the polarization is spin down. When $(\Sigma_n w_{\uparrow,n} < \Sigma_n w_{\downarrow,n})$ there are more $|\downarrow\rangle$ states eliminated from the ensemble and the polarization is spin up.

Consider the spin-selection rules for each of the trion states in Fig. 5. Clearly for the s-shell singlet trion (S_s), a σ^+ pulse only excites $|\uparrow\rangle$, giving a spin-down polarization. The triplet p-shell trion (T_p) consists of three closely spaced

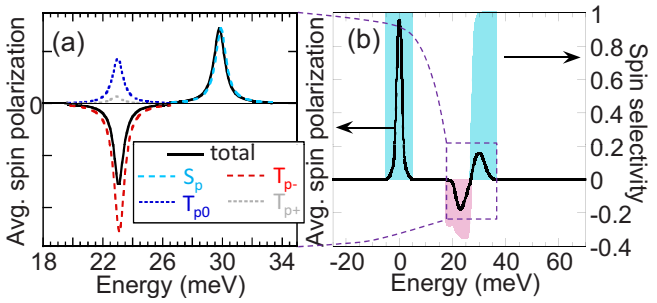

FIG. 6. (Color online) (a) Average resident electron spin polarization generated through p-shell trion states for a subensemble of identical QDs. (b) Average resident electron spin polarization and spin selectivity for s-shell and p-shell trions in an inhomogeneous ensemble. Energies are relative to the s-shell trion S_s. Selectivity is only plotted for energies where there is significant trion absorption.

states split by the electron-hole exchange interaction $(\Delta_{eh} \sim 200\ \mu\text{eV})$,[15] $|T_{p+}\rangle$, $|T_{p0}\rangle$, and $|T_{p-}\rangle$, with the subscripts $(0, \pm)$ corresponding to the projection of the total electron spin along z $(m_z = 0, \pm 1)$. Each state is further characterized by the hole-spin direction, leading to the six levels displayed, four of which are optically active. At zero magnetic field, σ^+ light only couples $|\uparrow\rangle$ to $|T_{p0}\rangle$ and $|\downarrow\rangle$ to $|T_{p-}\rangle$, with dipole moments of $\mu_p/\sqrt{2}$ and μ_p, respectively. Since the electron Zeeman energy (50 μeV) is significantly smaller than Δ_{eh}, the Voigt magnetic field has little effect on these states. They do become somewhat mixed, allowing a small dipole moment for the $|\uparrow\rangle$ to $|T_{p+}\rangle$ transition with σ^+ light. Since the optical pulses have a bandwidth of ~1 meV, any one of these triplet states can be excited for pulses in this photon energy range. Summing over each transition should give a net $|\uparrow\rangle$ polarization due to the larger dipole for $|T_{p-}\rangle$.

The singlet p-shell trion (S_p) state is expected to be higher in energy by several meV due to Δ_{ee}.[29,30] For σ^+ pulses, the $|\uparrow\rangle$ to $|S_p\rangle$ transition is allowed with a dipole moment of $\mu_p/\sqrt{2}$. Figure 6(a) plots the calculated spin polarization due to these triplet and singlet p-shell trions as a function of the excitation energy (relative to S_s) for a single QD. The $|\downarrow\rangle$ state is shown as a positive spin polarization for easier comparison to experimental data. The triplet states give a net negative signal and the singlet state gives a positive signal of equal amplitude. Note that the linewidth of the features is expected to be largely determined by the pulse bandwidth instead of the trion linewidths.

The QDs are modeled by anisotropic 2D harmonic potentials. The electrons and holes are described by Fock-Darwin states (harmonic oscillators with lateral sizes a_x and a_y) in this potential. We choose a Gaussian distribution of sizes with central sizes that give the s-p splitting in the experiment. These geometric parameters determine all electron-electron and electron-hole Coulomb and exchange integrals. The analytical wave functions allow us to derive simple scaling relations between the Coulomb and exchange integrals in the excited states and those in the s shell. A typical s-shell electron-hole exchange energy, Δ_{eh} is known from experiments and theory to be in the range 50–100 μeV.[31] Using these values in our model we obtain Δ_{eh} in the p shell consistent with experimental values of ~200 μeV.[15] Also, the

average Δ_{ee} in the p shell derived in our model is consistent with typical experimental values of several millielectron volts.[29]

The effects of inhomogeneity are included in Fig. 6(b) for an ensemble of QDs. Only QDs with an S_s energy near the probe photon energy are used for calculating the spin polarization (similar to experiment). This inhomogeneous distribution broadens the features in Fig. 6(a) but the negative dip and positive peak are still quite apparent. Despite the inhomogeneous broadening, the spin selectivity, defined as $\Sigma_n(w_{\uparrow,n}-w_{\downarrow,n})/\Sigma_n(w_{\uparrow,n}+w_{\downarrow,n})$, is still high for most of these features. The selectivity normalizes the average spin polarization by the total absorption probability, such that a spin selectivity of 1 or −1 indicates that only spin-up or spin-down electrons, respectively, are excited to trion states. The spin selectivity is 1 for the s-shell and p-shell singlet features at 0 and 30 meV in Fig. 6(b), respectively, since these trions have clear spin-selection rules and are spectrally separated from other trion states. The spin selectivity is only about $-1/3$ for the p-shell triplet feature at 22 meV since there are three closely spaced states with different spin-selection rules.

Comparing the calculated spin polarization in Fig. 6(b) to the ellipticity in Fig. 3(b) gives some qualitative agreement between experiment and theory but in experiment there is clearly no negative dip. There are several possibilities for why this dip does not occur. First, if the dipole moments for $|T_{p0}\rangle$ and $|T_{p-}\rangle$ are closer to equal instead of differing by $\sqrt{2}$, the T_p contribution will vanish, leaving only the S_p contribution. Second, it is possible that the assumption that recombination does not affect the spin polarization is faulty, leading to differing degrees of spin polarization depending on the trion dynamics. One might also wonder if the $p \leftrightarrow s$ transitions help explain the feature at 30 meV but we do not find that these states account for the difference. Experiments in single QDs, where the different transitions can be identified more easily may help resolve this discrepancy.

IV. CONCLUSIONS

We have performed two-color time-resolved spectroscopy of spin dynamics in an ensemble of InAs QDs. When the probe is centered on s-shell trions, a strong signal from precessing electron spins is observed when pumping near the probe and about 30 meV above, consistent with p-shell trions. A similar resonance is observed when the pump and probe photon energies are reversed. These results indicate that electron spins can be directly polarized and detected using p-shell trions. This effect is possible due to the exchange splitting of triplet and singlet p-shell trions, which are expected to polarize electron spins in opposite directions. Using the p-shell trions for spin manipulation may be useful for controlling the spatial extent of the carrier wave function and for separating the wavelength of optical control pulses from the QD emission wavelength.

ACKNOWLEDGMENTS

We thank T. L. Reinecke and Sophia E. Economou for helpful suggestions on the manuscript. This work is supported by the U.S. Office of Naval Research.

[1] X. Xu, Y. Wu, B. Sun, Q. Huang, J. Cheng, D. G. Steel, A. S. Bracker, D. Gammon, C. Emary, and L. J. Sham, Phys. Rev. Lett. **99**, 097401 (2007).
[2] M. Atature, J. Dreiser, A. Badolato, A. Hogele, K. Karrai, and A. Imamoglu, Science **312**, 551 (2006).
[3] M. H. Mikkelsen, J. Berezovsky, N. G. Stoltz, L. A. Coldren, and D. D. Awschalom, Nat. Phys. **3**, 770 (2007).
[4] J. Berezovsky, M. H. Mikkelsen, N. G. Stoltz, L. A. Coldren, and D. D. Awschalom, Science **320**, 349 (2008).
[5] D. Press, T. D. Ladd, B. Zhang, and Y. Yamamoto, Nature (London) **456**, 218 (2008).
[6] A. Greilich, S. E. Economou, S. Spatzek, D. R. Yakovlev, D. Reuter, A. D. Wieck, T. L. Reinecke, and M. Bayer, Nat. Phys. **5**, 262 (2009).
[7] P. Ester, L. Lackmann, S. M. de Vasconcellos, M. C. Hubner, A. Zrenner, and M. Bichler, Appl. Phys. Lett. **91**, 111110 (2007).
[8] D. Kim, S. E. Economou, S. C. Badescu, M. Scheibner, A. S. Bracker, M. Bashkansky, T. L. Reinecke, and D. Gammon, Phys. Rev. Lett. **101**, 236804 (2008).
[9] S. E. Economou and T. L. Reinecke, Phys. Rev. B **78**, 115306 (2008).
[10] J. J. Finley, P. W. Fry, A. D. Ashmore, A. Lemaitre, A. I. Tartakovskii, R. Oulton, D. J. Mowbray, M. S. Skolnick, M. Hopkinson, P. D. Buckle, and P. A. Maksym, Phys. Rev. B **63**, 161305(R) (2001).
[11] I. E. Kozin, V. G. Davydov, I. V. Ignatiev, A. V. Kavokin, K. V. Kavokin, G. Malpuech, H.-W. Ren, M. Sugisaki, S. Sugou, and Y. Masumoto, Phys. Rev. B **65**, 241312(R) (2002).
[12] S. Cortez, O. Krebs, S. Laurent, M. Senes, X. Marie, P. Voisin, R. Ferreira, G. Bastard, J.-M. Gerard, and T. Amand, Phys. Rev. Lett. **89**, 207401 (2002).
[13] B. Urbaszek, R. J. Warburton, K. Karrai, B. D. Gerardot, P. M. Petroff, and J. M. Garcia, Phys. Rev. Lett. **90**, 247403 (2003).
[14] S. M. Ulrich, M. Benyoucef, P. Michler, N. Baer, P. Gartner, F. Jahnke, M. Schwab, H. Kurtze, M. Bayer, S. Fafard, Z. Wasilewski, and A. Forchel, Phys. Rev. B **71**, 235328 (2005).
[15] M. E. Ware, E. A. Stinaff, D. Gammon, M. F. Doty, A. S. Bracker, D. Gershoni, V. L. Korenev, S. C. Badescu, Y. Lyanda-Geller, and T. L. Reinecke, Phys. Rev. Lett. **95**, 177403 (2005).
[16] A. Babinski, M. Potemski, S. Raymond, J. Lapointe, and Z. R. Wasilewski, Phys. Status Solidi C **3**, 3748 (2006).
[17] I. V. Ignatiev, S. Y. Verbin, I. Y. Gerlovin, R. V. Cherbunin, and Y. Masumoto, Opt. Spectrosc. **106**, 375 (2009).
[18] V. K. Kalevich, I. A. Merkulov, A. Y. Shiryaev, K. V. Kavokin, M. Ikezawa, T. Okuno, P. N. Brunkov, A. E. Zhukov, V. M. Ustinov, and Y. Masumoto, Phys. Rev. B **72**, 045325 (2005).
[19] S. Laurent, M. Senes, O. Krebs, V. K. Kalevich, B. Urbaszek, X. Marie, T. Amand, and P. Voisin, Phys. Rev. B **73**, 235302 (2006).

[20] Z. R. Wasilewski, S. Fafard, and J. P. McCaffrey, J. Cryst. Growth **201-202**, 1131 (1999).
[21] A. Greilich, D. R. Yakovlev, A. Shabaev, A. L. Efros, I. A. Yugova, R. Oulton, V. Stavarache, D. Reuter, A. Wieck, and M. Bayer, Science **313**, 341 (2006).
[22] S. G. Carter, A. Shabaev, S. E. Economou, T. A. Kennedy, A. S. Bracker, and T. L. Reinecke, Phys. Rev. Lett. **102**, 167403 (2009).
[23] A. Shabaev, A. L. Efros, D. Gammon, and I. A. Merkulov, Phys. Rev. B **68**, 201305(R) (2003).
[24] S. E. Economou, R.-B. Liu, L. J. Sham, and D. G. Steel, Phys. Rev. B **71**, 195327 (2005).
[25] M. V. G. Dutt, J. Cheng, B. Li, X. Xu, X. Li, P. R. Berman, D. G. Steel, A. S. Bracker, D. Gammon, S. E. Economou, R.-B. Liu, and L. J. Sham, Phys. Rev. Lett. **94**, 227403 (2005).
[26] R. Oulton, A. Greilich, S. Y. Verbin, R. V. Cherbunin, T. Auer, D. R. Yakovlev, M. Bayer, I. A. Merkulov, V. Stavarache, D. Reuter, and A. D. Wieck, Phys. Rev. Lett. **98**, 107401 (2007).
[27] A. S. Bracker, E. A. Stinaff, D. Gammon, M. E. Ware, J. G. Tischler, A. Shabaev, A. L. Efros, D. Park, D. Gershoni, V. L. Korenev, and I. A. Merkulov, Phys. Rev. Lett. **94**, 047402 (2005).
[28] Excitation of trion superposition states has also been considered but it has little effect on the electron spin polarization.
[29] R. J. Warburton, C. Schaflein, D. Haft, F. Bickel, A. Lorke, K. Karrai, J. M. Garcia, W. Schoenfeld, and P. M. Petroff, Nature (London) **405**, 926 (2000).
[30] R. Ferreira and G. Bastard, Appl. Phys. Lett. **74**, 2818 (1999).
[31] M. Bayer, G. Ortner, O. Stern, A. Kuther, A. A. Gorbunov, A. Forchel, P. Hawrylak, S. Fafard, K. Hinzer, T. L. Reinecke, S. N. Walck, J. P. Reithmaier, F. Klopf, and F. Schäfer, Phys. Rev. B **65**, 195315 (2002).